AD

USAAMRDL TECHNICAL REPORT 71-70

MATERIAL NONLINEARITY EFFECTS IN OPTIMIZATION CONSIDERATIONS OF STIFFENED CYLINDERS AND INTERPRETATION OF TEST DATA SCATTER FOR COMPRESSIVE BUCKLING

By

J. Mayers

E. Meller

March 1972

EUSTIS DIRECTORATE
U. S. ARMY AIR MOBILITY RESEARCH AND DEVELOPMENT LABORATORY
FORT EUSTIS, VIRGINIA

CONTRACT DAAJ02-70-C-0075
DEPARTMENT OF AERONAUTICS AND ASTRONAUTICS
STANFORD UNIVERSITY
STANFORD, CALIFORNIA

62

DISCLAIMERS

The findings in this report are not to be construed as an official Department of the Army position unless so designated by other authorized documents.

When Government drawings, specifications, or other data are used for any purpose other than in connection with a definitely related Government procurement operation, the United States Government thereby incurs no responsibility nor any obligation whatsoever; and the fact that the Government may have formulated, furnished or in any way supplied the said drawings, specifications, or other data is not to be regarded by implication or otherwise as in any manner licensing the holder or any other person or corporation, or conveying any rights or permission, to manufacture, use, or sell any patented invention that may in any way be related thereto.

Trade names cited in this report do not constitute an official endorsement or approval of the use of such commercial hardware or software.

DISPOSITION INSTRUCTIONS

Destroy this report when no longer needed. Do not return it to the originator.

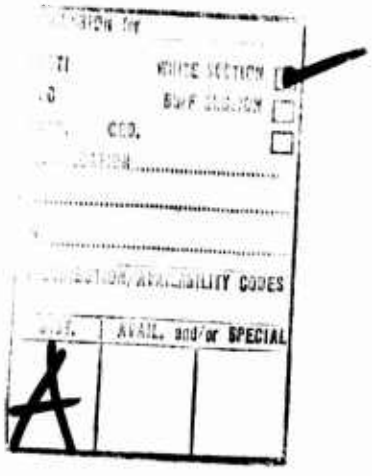

UNCLASSIFIED

Security Classification

DOCUMENT CONTROL DATA - R & D

(Security classification of title, body of abstract and indexing annotation must be entered when the overall report is classified)

1. ORIGINATING ACTIVITY (Corporate author)	2a. REPORT SECURITY CLASSIFICATION
Stanford University Department of Aeronautics and Astronautics Stanford, California	Unclassified
	2b. GROUP N/A

3. REPORT TITLE

MATERIAL NONLINEARITY EFFECTS IN OPTIMIZATION CONSIDERATIONS OF STIFFENED CYLINDERS AND INTERPRETATION OF TEST DATA SCATTER FOR COMPRESSIVE BUCKLING

4. DESCRIPTIVE NOTES (Type of report and inclusive dates)

Final Technical Report

5. AUTHOR(S) (First name, middle initial, last name)

J. Mayers
E. Meller

6. REPORT DATE	7a. TOTAL NO. OF PAGES	7b. NO. OF REFS
March 1972	60	48

8a. CONTRACT OR GRANT NO.	9a. ORIGINATOR'S REPORT NUMBER(S)
DAAJ02-70-C-0075 b. PROJECT NO. 1F061102A33F02 c. d.	USARMDL Technical Report 71-70
	9b. OTHER REPORT NO(S) (Any other numbers that may be assigned this report)

10. DISTRIBUTION STATEMENT

Approved for public release; distribution unlimited.

11. SUPPLEMENTARY NOTES	12. SPONSORING MILITARY ACTIVITY
	Eustis Directorate U.S. Army Air Mobility R & D Laboratory Fort Eustis, Virginia

13. ABSTRACT

A limited optimization study is undertaken of imperfect, eccentrically stiffened 2024-T3 aluminum alloy cylinders under axial compression based on (1) a linear theory with applied buckling load reduction factors to account for initial imperfections and inelasticity and (2) a kinematically and constitutively nonlinear maximum strength analysis. The latter is shown to be less conservative for the most efficient design: combined stringer- and ring-stiffening. Credibility of the maximum strength approach is demonstrated through its use in correlating experimental results obtained for 10- and 14-in. diameter steel cylinders having different proportional-limit stresses, respectively. Finally, material nonlinearity is shown to offer a plausible qualitative explanation for a significant amount of the scatter in axial compression tests for cylinders with radius-to-thickness ratios of practical interest.

DD FORM 1 NOV 68 1473 REPLACES DD FORM 1473, 1 JAN 64, WHICH IS OBSOLETE FOR ARMY USE.

UNCLASSIFIED

Security Classification

14. KEY WORDS	LINK A		LINK B		LINK C	
	ROLE	WT	ROLE	WT	ROLE	WT
Stiffened Shells						
Maximum Strength						
Failure Analysis						
Design Optimization						
Plasticity						
Axial Compression Loading						

DEPARTMENT OF THE ARMY
U. S. ARMY AIR MOBILITY RESEARCH & DEVELOPMENT LABORATORY
EUSTIS DIRECTORATE
FORT EUSTIS, VIRGINIA 23604

This program was carried out under Contract DAAJ02-70-C-0075 with Stanford University.

The report presents the results of research conducted to evaluate nonlinearity effects in the optimization of imperfect, eccentrically stiffened cylinders under axial compression. A kinematically and constitutively nonlinear maximum strength analysis technique is used. Results with this approach appear to be more meaningful than the linear theory with load reduction factors.

This report has been reviewed by this Directorate and is considered to be technically sound. It is published for the exchange of information and the stimulation of future research.

The technical monitor for this program was Mr. James P. Waller, Structures Division.

Task 1F061102A33F02
Contract DAAJ02-70-C-0075
USAAMRDL Technical Report 71-70
March 1972

MATERIAL NONLINEARITY EFFECTS IN OPTIMIZATION CONSIDERATIONS OF STIFFENED CYLINDERS AND INTERPRETATION OF TEST DATA SCATTER FOR COMPRESSIVE BUCKLING

Final Report

By

J. Mayers
E. Meller

Prepared by

Department of Aeronautics and Astronautics
Stanford University
Stanford, California

for

EUSTIS DIRECTORATE
U. S. ARMY AIR MOBILITY RESEARCH AND DEVELOPMENT LABORATORY
FORT EUSTIS, VIRGINIA

II

ABSTRACT

A limited optimization study is undertaken of imperfect, eccentrically stiffened 2024-T3 aluminum alloy cylinders under axial compression based on (1) a linear theory with applied buckling load reduction factors to account for initial imperfections and inelasticity and (2) a kinematically and constitutively nonlinear maximum strength analysis. The latter is shown to be less conservative for the most efficient design: combined stringer- and ring-stiffening. Credibility of the maximum strength approach is demonstrated through its use in correlating experimental results obtained for 10- and 14-in. diameter steel cylinders having different proportional-limit stresses, respectively. Finally, material nonlinearity is shown to offer a plausible qualitative explanation for a significant amount of the scatter in axial compression tests for cylinders with radius-to-thickness ratios of practical interest.

FOREWORD

The work reported herein constitutes a portion of effort being undertaken at Stanford University for the Eustis Directorate, U. S. Army Air Mobility Research and Development Laboratory under Contract DAAJ02-70-C-0075 (Task 1F061102A33F02). The present program is one in a series aimed at establishing accurate theoretical prediction capability for the static and dynamic behavior of aircraft structural components using both conventional and unconventional materials. Predecessor contracts supported investigations which led, in part, to the results presented in Reference 10, 11, 23, 36, 40, 42, and 43.

For his part in assisting with digital computer calculations, the efforts of Mr. Joseph Mullen, Jr., are gratefully acknowledged.

TABLE OF CONTENTS

LIST OF ILLUSTRATIONS

LIST OF SYMBOLS

A	cross-sectional area of stiffening element, $in.^2$
A_{ij}	nondimensional direct stress coefficient
a_{ij}, b_{ij}, c_{ij}	nondimensional bending stress coefficients
C	nondimensional buckling stress coefficient, $\sigma R/Et$
$\bar{C}$	nondimensional eccentricity constant
D	bending stiffness of isotropic cylinder, $D = \frac{Et^3}{12(1-\nu^2)}$, lb-in.
D_1, D_2, D_3, D_4	orthotropic shell nondimensional flexural stiffness constants
D_x, D_y	bending stiffnesses of orthotropic cylinder in x- and y-directions, respectively, lb-in.
D_{xy}	twisting stiffness of orthotropic cylinder, lb-in.
d	stringer spacing, in.
E	Young's modulus, psi
E_1, E_2, E_3, E_4	orthotropic shell nondimensional extensional stiffness constants
E_T	tangent modulus, psi
E_S	secant modulus, psi
E_x, E_y	extensional stiffnesses of orthotropic cylinder in x- and y-directions, respectively, lb/in.
e	unit end shortening, in./in.
G	shear modulus, psi

G_{xy}	midsurface shear stiffness of orthotropic cylinder, lb/in.
h_x, h_y	distances separating the faces of two-element, orthotropic cylinder in x- and y-directions, respectively, in.
h_{xy}	fictitious weighted average of h_x and h_y, in.
I	moment of inertia of stiffening element about its centroid, $in.^4$
J	torsional stiffness constant for stiffening element, $in.^4$
K	nondimensional Ramberg-Osgood material constant
L	length of cylinder, in.
ℓ	ring spacing, in.
M_x, M_y	bending moments per unit length in x- and y-directions, respectively, lb
M_{xy}	twisting moment per unit length, lb
m	number of axial waves
N	nondimensional Ramberg-Osgood material constant
n	number of circumferential waves
R	radius of cylinder, in.
$\bar{R}$	nondimensional extensional stiffness ratio for ring, $\bar{R} = \frac{E_r A_r}{Et\ell}$
$\bar{S}$	nondimensional extensional stiffness ratio for stringer, $\bar{S} = \frac{E_s A_s}{Etd}$

t	thickness of homogeneous, isotropic cylinder, in.
t_f	thickness of face sheet of two-element cylinder, in.
$\bar{t}_x$	effective thickness of orthotropically stiffened cylinder in axial direction, $\bar{t}_x = \frac{A_s}{d} + t$, in.
U''	Reissner functional, lb-in.
u,v,w	displacements of point on middle surface of cylinder in x-, y-, and z-directions, respectively, in.
w_0	initial deviation of midsurface displacement in radial direction, in.
x,y,z	cylinder coordinates, in.
$\bar{z}$	distance from centroid of stiffening element to middle surface of cylinder, in.
γ_{xy}	total shear strain in the xy-plane, in./in.
γ'_{xy}	shear strain at middle surface, in./in.
γ''_{xy}	shear strain due to twisting, in./in.
ϵ	uniaxial strain, in./in.
ϵ_{eff}	effective strain, in./in.
ϵ_x, ϵ_y	total strains in x- and y-directions, respectively, in./in.
ϵ'_x, ϵ'_y	strains due to extension in x- and y-directions, respectively, in./in.
$\epsilon''_x, \epsilon''_y$	strains due to bending in x- and y-directions, respectively, in./in.

η	nondimensional wave parameter, $\eta = n^2(\bar{t}_x/R)$; plasticity reduction factor, $\sqrt{(E_T E_S)/E^2}$
λ_x, λ_y	buckle half-wavelengths in x- and y-directions, respectively, in.
μ	nondimensional buckle aspect ratio, $\mu = \lambda_y/\lambda_x$
μ_x, μ_y	nondimensional Poisson's ratios for extension of orthotropic cylinder in x- and y-directions, respectively
ν	nondimensional Poisson's ratio for isotropic cylinder
ν_x, ν_y	nondimensional Poisson's ratios for bending of orthotropic cylinder in x- and y-directions, respectively
ξ_{ij}	nondimensional displacement coefficient
ξ_{ij}	nondimensional imperfection amplitude coefficient
σ	average compressive stress; uniaxial stress, psi
σ_{eff}	effective stress, psi
σ_x, σ_y	total stresses in x- and y-directions, respectively, psi
σ'_x, σ'_y	average direct stresses in x- and y-directions, respectively, psi
σ''_x, σ''_y	bending stresses in x- and y-directions, respectively, psi
τ_{xy}	total shear stress in xy-plane, psi
τ'_{xy}	average shear stress in xy-plane, psi
τ''_{xy}	shear stress due to twisting, psi

SUBSCRIPTS

b	denotes bottom face of two-element model
cr	critical
e	experimental
eff	effective
f	denotes face sheet
i,j	integers
max	maximum
0	denotes initial radial imperfection amplitudes
pl	proportional limit
r,s	denotes rings and stringers, respectively
t	denotes top face of two-element model
x,y,z	denotes longitudinal, circumferential, and radial directions, respectively

INTRODUCTION

The post-World War II developments in aircraft design leading to greatly increased performance and capability can be attributed more to breakthroughs in the areas of propulsion and aerodynamics than to advances in structures. With weight-consciousness becoming ever more prevalent, it is interesting that the primary source of vehicle empty weight, the load-carrying structure, continues to evidence prejet-age design considerations. Much optimism has been placed in the potential of composite materials for improving structural efficiency. However, the promise of composites notwithstanding, conventional sheet-stringer construction continues to form the basic structure of fuselages, wings, and empennages in general; thus, it offers a logical and attractive area for fundamental weight reduction, with possible cascading effects relative to the overall system either in decreased weight or weight tradeoffs.

In conventional aircraft construction, the thin curved plate or shell is the key element. Yet the design of such elements, especially for stiffness considerations, continues to be founded upon semiempirical and, apparently, overconservative criteria. The buckling of thin shells in compression is a case in point. The unfortunate lack of experimental data to guide the development of satisfactory design procedures for practical shells is emphasized by Peterson in Reference 1. Additionally, the frustration underlying the myriad attempts to resolve the thin shell buckling problem satisfactorily from a theoretical standpoint is evidenced in the remarks of Almroth et al. in Reference 2 as justification for the need to establish approximate methods of stability analysis leading to design criteria which are less conservative than those in common usage but which can still be employed with a high degree of confidence.

Much has been made of the deleterious effects of initial imperfections, boundary conditions, and prebuckling deformations in the buckling of shells under compressive loading in attempts to explain the significant

discrepancy between the 60-year-old classical theory and experiments of the past 50 years (see, for example, the survey papers of Hoff,[3,4] Stein[5], and Hutchinson and Koiter[6]). The consensus leans heavily toward initial imperfections as the significant degrading factor compared to the influences of boundary conditions and prebuckling deformations. The importance for design purposes attributed to initial imperfections in the buckling of thin-walled shells in compression is reflected in recommended criteria appearing in handbooks either developed or sponsored by the National Aeronautics and Space Administration.[7,8,9] Also, one of the most recent of design criteria advanced for axially loaded cylindrical shells makes generous use of an empirical factor to account for the presence of initial imperfections in practical shells.[2]

Although from time to time the question of nonlinear elastic and offset plastic (yielding) buckling has arisen, the tendency has been to treat the buckling of thin-walled highly curved plates and shells on the basis of mathematical models using linear stress-strain laws. Plastic buckling of shells is more appropriate to thick shells and of little interest to aircraft shell designers and analysts. Very thin shells, wherein linear elastic material behavior at buckling is more prone to occur, is again of diminished interest in design because of the large penalties to be paid for imperfection-sensitivity "knockdown" factors and loss of aerodynamic smoothness due to the catastrophic nature of thin shell buckling. In the range of "effectively thick" shells (closely stiffened and sandwich construction), however, the imperfection sensitivity is significantly less. But, it is in this range that practical configurations exist (closely spaced, moderately heavy stiffening and sandwich concepts), and their buckling loads cannot be determined independently of nonlinear material behavior if structural efficiency is to be achieved subject to the usual condition that no yielding take place at limit load. Mayers and Wesenberg[10,11] have called attention to the importance of nonlinear material behavior in the failure mechanism of imperfect, axially compressed, conventional,

stiffened, and sandwich shells, especially in the range of practical interest for both material properties and geometric parameters.

It is the purpose of the present study to demonstrate how the maximum strength analysis can be used to optimize in a broad sense an initially imperfect, eccentrically stiffened, aluminum cylinder. The results are compared with the more common procedure in Reference 9. Additionally, credibility of the maximum strength concept, theory, and analysis is demonstrated by application to several of the steel test-cylinder configurations reported in Reference 12; these cases serve as an explanation of the apparently anomalous cylinder behavior appearing in the presentation of results in Reference 12 under the assumption that all buckling failures occurred with linear elastic material behavior. Finally, the overall implication of the present investigation and its forerunners[10,11] possibly sheds new light on interpretation of the results of the perceptive pioneering work performed by Donnell[13] and Lundquist[14] both theoretically and experimentally on the compressed shell buckling problem almost 40 years ago and, apparently, too soon overlooked by myriad investigators concerned with mathematical solutions of the classical small- and large-deflection theories for linear elastic shells, including such effects as initial imperfections, combinations of boundary conditions, and prebuckling deformations.

DISCUSSION AND RESULTS

TYPICAL DESIGN PROCEDURE

The buckling phenomenon attributed to shells under compressive loading has been commonly treated in analysis and design as classical bifurcation buckling with empirically and theoretically established reduction factors applied to the classical buckling loads to account for the significant discrepancies that invariably exist between theory and experience. The classical axial compression buckling loads for circular orthotropic shells with closely spaced, eccentric stiffening can be obtained, for example, from the initial developments of Baruch and Singer[15] and the broad generalization accomplished by Block et al.[16] For symmetric stiffening, the Baruch-Singer buckling criterion reduces to that of Stein and Mayers[17] for orthotropic, circularly curved sandwich plates and shells when transverse shear effects are neglected. The latter, in turn, again with transverse shear effects neglected, reduces to the classical buckling load for homogeneous, isotropic, long thin shells developed independently by Lorenz,[18] Timoshenko,[19] and Southwell[20] some 60 years ago. For such cylinders, prediction and experience have finally been closely matched by very careful fabrication and testing techniques.[21,22,23,24] Although the specimens involved must be considered as much too small for practical applications, they, nevertheless, served to expose initial imperfections as a main contributor to the discrepancy between classical theory and experiment as well as to explain the cause of some of the significant scatter existing in a very large body of test data.

Buckling Load "Knockdown" Factors

One of the most scrupulous attempts to establish a consistent "knockdown" factor curve as a function of radius-to-thickness ratio for use in design is evidenced by the work of Weingarten et al.[25] The curve for axially compressed cylinders presented in Reference 25 represents the lower bound to selected buckling-load data on unstiffened shells

garnered from a host of sources. Available data were eliminated from consideration when, for example, the test results were believed to reflect the influence of boundary conditions, poor fabrication and testing techniques, and average stress levels in excess of 70% of material yield stress. The selection process notwithstanding, the group of data leading to the lower bound design curve still presents a considerable scatter band at any radius-to-thickness ratio, not all of which in the opinion of Weingarten et al. can be isolated to the effects of initial imperfections. The design curve of Reference 25 is essentially the same as those appearing in the NASA handbooks[7,8,9] for use with unstiffened cylinders. Careful attempts have also been made to explain the significant scatter band obtained with stiffened cylinders (see, for example, the study by Peterson in Reference 1). After such considerations as prebuckling deformations, discreteness (versus smearing) of stiffening elements, and fabrication tolerances, the presence of imperfections, residual stresses, and local skin buckling are the leading reasons advanced for the lack of correlation between classical theory predictions and experiments relative to compressed shells. Unfortunately, the number of stiffened-cylinder tests reported in the literature is miniscule compared with that for unstiffened cylinders; further, as pointed out by Peterson,[1] there are no available data on conventional ring- and stringer-stiffened cylinders in which local skin buckling does not precede general buckling.

Alternate Procedure

In the case of either stiffened or unstiffened shells under compression, there has developed more recently an alternative approach to that of applying suitable reduction factors to the classical buckling load. This approach stems from the Koiter theory for the elastic buckling and initial postbuckling of imperfect thin shells.[26] In Koiter-type analyses,[27,28] the calculated buckling load inherently accounts for the presence of an imperfection distribution over the shell surface corresponding to the axisymmetric classical buckling mode. The imperfection distribution possesses an arbitrary amplitude which can be

selected to yield correlations with empirically established "knockdown" factor versus effective-radius-to-thickness curves as suggested by, for example, Madsen and Hoff[29] and Almroth et al.[2] However, in Reference 2 arguments are presented for limiting the usefulness of the Koiter theory in practical analysis at the present time.

Effectively Thick Cylinders

In the light of the discussion to this point, it is obvious that the presence of initial imperfections is the main cause of the discrepancy between prediction and experiment for thin shells under compressive loading. However, the effect of imperfections tends to diminish as the radius-to-thickness ratio is decreased. Stiffened and sandwich shells of practical dimensions are by nature in the "effectively thick" category. Whereas unstiffened shells can have "knockdown" factors applied to the classical buckling loads approaching 0.20, it has been suggested that shells with closely spaced, moderately heavy stiffening may be designed with a "knockdown" factor of 0.75 applied to the classical buckling load as long as the material remains linear elastic and no local skin buckling precedes general instability (see Reference 9). Further, the extensive experimental work of Singer et al.[30,31,32] has given rise to the contention that practical stiffened shells tend to behave reasonably closely indeed to the classical theory and that a sufficiently conservative reduction factor for linear elastic material behavior lies at about the 0.75 level. Also, Hoff in Reference 4 has commented to the effect that the classical theory for orthotropic shells is probably sufficiently accurate for engineering calculations when the effective-radius-to-thickness ratio of the stiffened cylinder is equal to or less than 200.

MAXIMUM STRENGTH CONSIDERATIONS

To the designer concerned with weight problems in shell structures, there is little comfort in a status quo which leaves the satisfactory predictions of buckling loads under compression unresolved theoretically

and no other choices than either the use of semiempirical criteria which are admittedly still conservative or design by test, a costly if not prohibitive procedure. Since the cylindrical shell buckling problem has been treated in at least 1600 references[6] and still poses a challenge even in the homogeneous, isotropic case, it seems quite reasonable to consider another facet of the physical behavior at buckling which has been almost deliberately avoided for as long as experiments have failed to demonstrate the predictions of the classical theory. This facet has to do with the role that nonlinear material behavior may play in the shell buckling process. The buckling load of a compressed shell is in reality the maximum or failure load. To deal with the failure mechanism on the basis of linear elastic material behavior, especially in "effectively thick" shells of the stiffened or sandwich type which if devoid of initial imperfections would undergo buckling without yielding, is questionable. Perhaps preoccupation with postbuckling behavior of very thin shells at large deflections and correlation of minimum postbuckling equilibrium stresses with the low buckling stresses of actual cylinders turned attention away from the maximum strength problem. Or perhaps preoccupation with imperfection sensitivity of compressed shells kept attention centered qualitatively in this area. Imperfect shells buckling in the yield region have been discussed by Batterman[33] and Hutchinson;[34] however, this type of problem concerns thick shells and cannot be considered representative of the aircraft shell design problem. Remarkably, Donnell[13] in his earliest work on the buckling of imperfect, thin shells in compression developed a design formula which based failure on the arbitrary criterion of the maximum stress at buckle nodes reaching the yield stress of the material. Had this concept of thin shell failure been pursued more vigorously, it is possible that the succeeding more accurate large-deflection analyses of shells would not have been restricted to linear material behavior for so many years.

In the course of investigating the accuracy of von Kármán-Donnell[35] shell theory for studying the axial compression postbuckling problem of thin shells, Mayers and Rehfield[36] and Hoff, Madsen, and Mayers[37] in

complementary efforts brought an end to the search for the minimum postbuckling stress a thin shell can support. The former concluded as well that the shell postbuckling problem could not be resolved satisfactorily on the basis of linear elastic material behavior. Subsequent investigations by Mayers and Wesenberg[10,11] of the nonlinear behavior of initially imperfect, axially compressed unstiffened, stiffened, and sandwich shells in the initial buckling region (maximum strength problem) have yielded indisputable evidence that the maximum load can be strongly dependent upon the combined effects of initial imperfections and the loss of the classical linear relationship between stress and strain given by Hooke's law. The phenomenon is pronounced in either closely stiffened shells with moderately heavy stiffening or sandwich cylinders ("effectively thick" practical construction) using materials that are described by the lower exponents in the Ramberg-Osgood[38] representation of uniaxial stress-strain curves for aircraft structural metals. Materials in which the uniaxial stress-strain curve exhibits little range of persisting initial modulus include stainless steel, nickel, copper, brass, and nonferrous superalloys; annealed metals in general; metals at elevated temperature; and, to a large extent, filamentary composites with high-performance fibers.

Optimization Considerations

Normally, in the design process using, for example, the criteria of Reference 9, a stiffened or sandwich cylinder is assumed to be geometrically perfect and in a state of uniform compressive stress at the instant of buckling (bifurcation). The possibility of buckling at stresses exceeding the proportional limit stress is accounted for by applications of a reduced modulus after Gerard.[39] Then, the presence of initial imperfections in the shell is recognized by applying a suitable "knockdown" factor obtained from an empirical design curve such as that of Weingarten et al.[25] It is important to note, as pointed out in References 10 and 11, that nonlinear material behavior is not an unusual occurrence in imperfect shells undergoing bending and initial buckling (maximum strength) even though the average compressive stress

remains in the linear elastic range. Also, it should be borne in mind that the use of a reduced modulus in the "handbook" approach does not necessarily imply that yielding in the design sense (0.2% offset yield stress) has taken place. Thus, it is still moot whether or not the commonly used design procedure based upon a gross idealization of compressed shell buckling behavior is realistic. Presumably, the procedure is well on the conservative side and, therefore, justifiable.

Now, where structural efficiency is concerned, the degree of conservatism is important. The justification for the relatively new design procedure presented in Reference 2 is that, although based upon semi-empirical considerations, in the absence of satisfactory theory, it yields, nevertheless, the same or less conservative results than other methods in use. For a maximum strength (failure) analysis of an initially imperfect, stiffened shell, it would appear that bending, buckling, and postbuckling in a nonlinear elastic sense prior to yielding is more representative of the actual physical behavior than either (1) the classical idealization of a perfect shell with correction factors to account for both initial imperfections and nonlinear material behavior applied in a gross sense or (2) prediction of the reduced buckling load based upon a linear material, initial postbuckling analysis which takes into account the first-order effects of an axisymmetric imperfection pattern, the amplitude of which is correlated with empirical curves of "knockdown" factor versus radius-to-effective-thickness ratio for axially compressed cylinders. Which of the approaches leads to a more realistic estimate of compressed shell behavior for optimization considerations and the evaluation of test data is the basis of the study results to follow. The study itself is based upon the theoretical developments presented in References 10, 11, and 40 which, in turn, are outgrowths of the investigations reported in References 41, 42, and 43. In the latter studies, compressed plates were of interest; Reference 43 presents the essentially exact solution to the maximum strength of postbuckled rectangular plates and places the well-known von Kármán effective width formula[44] in proper perspective.

As a basis for a necessarily limited optimization study, the longer of the two 2024-T3 aluminum alloy, integral, externally, longitudinally stiffened cylinder cross sections used in the experimental investigation of Card and Jones[45] is adopted for the reference case; it appears in Figure 1 as Case 0 . The uniaxial stress-strain curve for 2024-T3 aluminum alloy is shown in Figure 2. Although no attempt appears to have been made in the program of Reference 45 to consider the problem of cylinder optimization, the stringers were apparently sized and located to preclude local buckling in view of the fact that none occurred. The actual cylinder behaved as if it were "effectively thick", since the experimental result was 92% of the calculated classical value. This is reasonable as the effective radius-to-thickness ratio for Case 0 is only 167 . As shown in Reference 10, aluminum cylinders under compression begin to exhibit the effects of stress-strain curve nonlinearity below about $(R/t)_{eff} = 200$. The test results of Reference 45 in the form of cylinder stress-strain curves bear out the fact that the reference cylinder was in the nonlinear range at maximum load. Thus, with the strain data indicating no local buckling prior to general buckling, the discrepancy between classical theory and experiment cannot be attributed to initial imperfections and boundary conditions alone.

Now, under the hypothetical design consideration that no yielding (0.2% offset definition) shall occur at limit load, the buckling stress in the cylinder can be raised appreciably even though the nonlinear portion of the stress-strain curve below the yield stress is involved. On the basis of simply supported ends, the Baruch/Singer-NASA[15,16] uniform compression buckling criterion yields 18.6 ksi for Case 0 as indicated in Table I; for Cases 1, 2, and 3, the results are seen to be 31.5, 31.4, and 40.1 ksi, respectively. Each of the latter three cases is in the nonlinear elastic range (nonlinear elastic and inelastic are used interchangeably for convenience below the yield stress) and a common design procedure (see, for example, Reference 9) is to apply a plasticity correction factor or reduced modulus ($\eta = \sqrt{(E_T E_S)/E^2}$) to

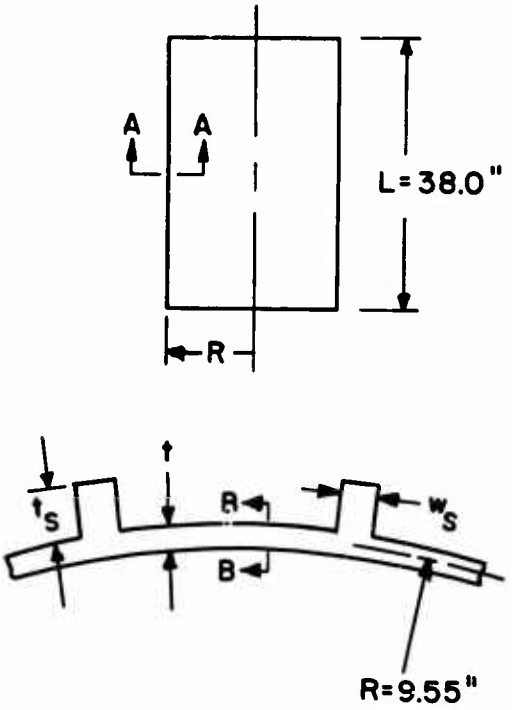

SECTION A-A

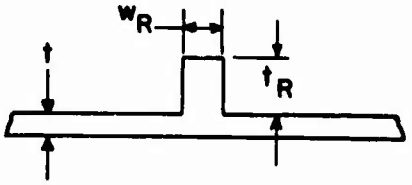

SECTION B-B

CASE	NUMBER		t	w_S	t_S	w_R	t_R
	STRINGERS	RINGS					
0	60	0	0.028	0.097	0.300	0	0
1	60	39	0.028	0.061	0.183	0.045	0.060
2	45	30	0.036	0.080	0.238	0.050	0.060
3	60	39	0.031	0.064	0.193	0.050	0.090

NOTE: ALL DIMENSIONS IN INCHES.

Figure 1. Cylinder Geometries of Optimization Study.

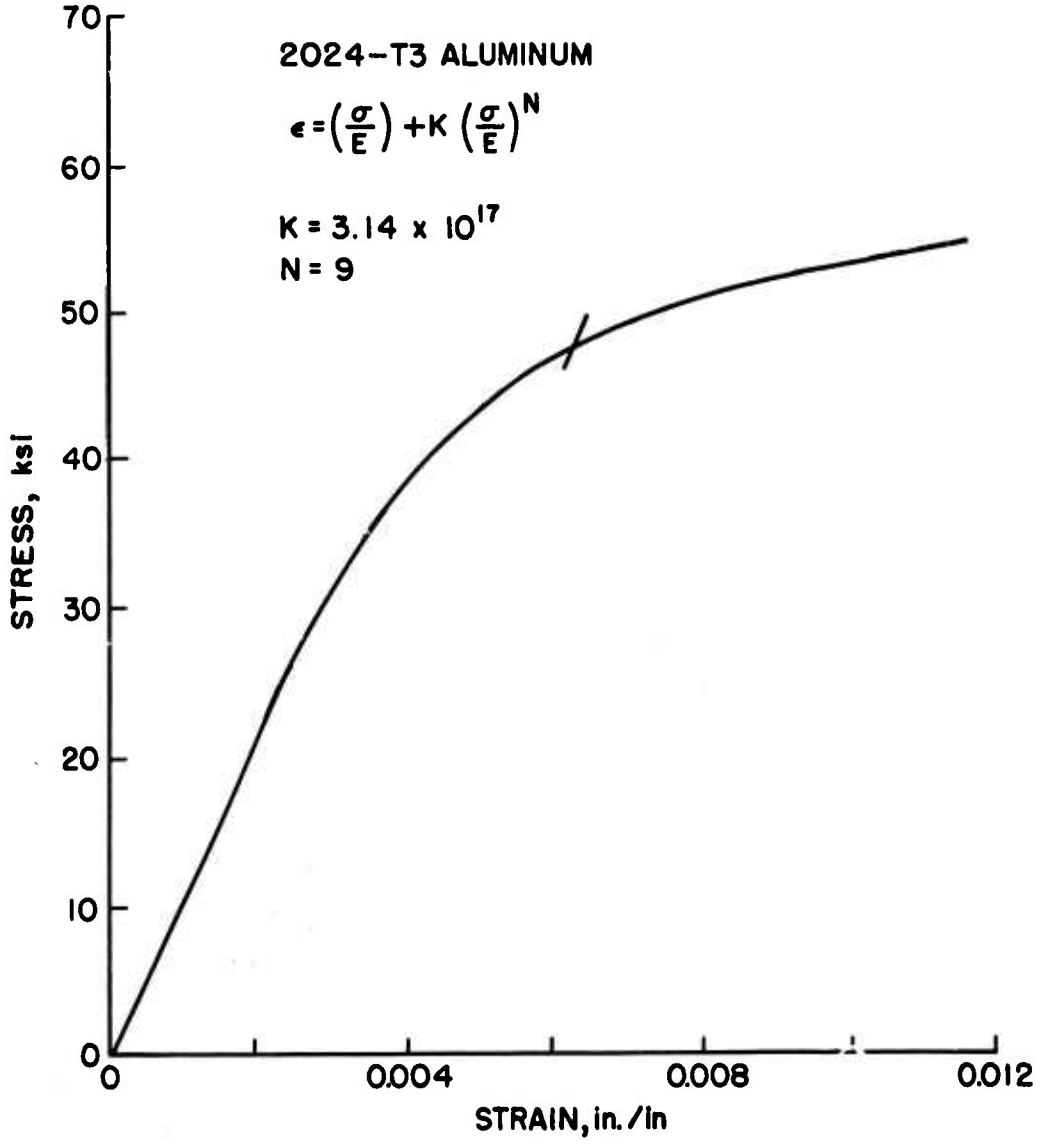

Figure 2. Stress-Strain Curve for 2024-T3 Aluminum.

TABLE I. COMPARISON OF BUCKLING STRESSES AND WEIGHTS

Case	$\sigma^{(1)}$ (ksi)	$\eta = \sqrt{(E_T E_S)/E^2}$	$\sigma^{(2)}$ (ksi)	$\sigma^{(3)}$ (ksi)	$\sigma^{(4)}$ (ksi)	$\xi_{11_0}{}^{(5)}$	Weight Ratio
0	18.6	1.00	18.6	13.9	18.5	$\simeq 0.4$	1.0
1	31.5	0.94	29.7	22.3	30.9	$\simeq 0.4$	0.74
2	31.4	0.94	29.6	22.2	30.9	$\simeq 0.5$	0.90
3	40.1	0.86	34.5	25.8	38.6	$\simeq 1.0$	0.84

(1) Baruch/Singer-NASA elastic buckling stress.

(2) Baruch/Singer-NASA elastic buckling stress multiplied by η .

(3) Baruch/Singer-NASA elastic buckling stress multiplied by 0.75 η .

(4) Present maximum strength analysis buckling stress for $\xi_{11_0} = 0.0001$.

(5) Magnitude of ξ_{11_0} required to reduce present maximum strength analysis buckling stress (based on $\xi_{11_0} = 0.0001$) by a factor of 0.75 .

the result. The corrected buckling stresses are shown in Table I along with the buckling stress predictions of the maximum strength theory and analysis outlined in Appendix I. In each case, an initial imperfection amplitude $\xi_{11_0} = 0.0001$ has been assumed in order to provide a loading path into the nonlinear elastic range. For Case 0, it may be noted that the Baruch/Singer-NASA[15,16] perfect cylinder criterion and the imperfect cylinder maximum strength analysis yield essentially the same result since the material behaves linearly and the imperfection amplitude ξ_{11_0} is so very small. For Cases 1, 2, and 3, however, the critical stresses obtained from the two markedly different approaches are in good agreement only for $\eta \simeq 1$. That is, in view of the stress levels involved, the Baruch/Singer-NASA values must be corrected for inelastic effects; the resulting inelastic buckling stresses are seen to be increasingly lower than the maximum-strength analysis counterparts as the linear elastic buckling stress levels increase. The discrepancy grows still further, Case 0 included, because the design recommendation of, say, Reference 9 includes a reduction of the Baruch/Singer-NASA buckling stresses by a factor of 0.75 to account for the possible presence of initial imperfections. The factor of 0.75 is recommended for closely spaced, moderately heavy stiffening; it becomes as small as 0.20 for unstiffened cylinders of relatively large radius-to-thickness ratio. Although it is true that the maximum strength analysis has been based upon an imperfection amplitude of $\xi_{11_0} = 0.0001$, the imperfection amplitude required to reduce each of the maximum strength analysis results by 0.75 (in consonance with the handbook recommendation) is unrealistic as indicated by the ξ_{11_0} values listed for each case in Table I. Since for unstiffened thin cylinders, values of $\xi_{11_0} > 0.1$ would imply unsatisfactory fabrication techniques, the Table I values, which are 4 to 10 times greater, show that the 0.75 "knockdown" factor is too conservative for application to all cylinders with closely spaced, moderately heavy stiffening, at least for 2024-T3 aluminum.

The weight of each cylinder referred to Case 0 is also shown in Table I. It can be seen that Case 1 is the lightest (- 26%) and carries almost 60% more stress than does the reference cylinder according to the

Baruch/Singer-NASA perfect cylinder, linear theory criterion corrected for inelasticity. By comparison, the maximum strength analysis shows that for $\xi_{11_0} = 0.0001$ (an essentially perfect cylinder), Case 1 carries about 67% more stress at buckling. On the other hand, the next lightest cylinder (- 16%), Case 3, supports 86% more stress according to the Baruch/Singer-NASA criterion corrected for inelasticity, but almost 110% more stress according to the maximum strength theory. The reason for this must be attributed to the plasticity correction factor η and the linear buckling theory assumption of a uniform stress state in the cylinder at the instant of buckling (bifurcation). At high stress levels and prior to reaching the material yield stress, the plasticity correction factor η can reflect very strongly the tangent modulus of the stress-strain curve and appreciably reduce the linear elastic bifurcation stress. It can be noted from Table I that the inelastic buckling stresses for Cases 1, 2, and 3 based upon the linear theory buckling criterion are closer together than in the purely linear-theory predictions; this is the result of the tangent modulus behavior at increasingly nonlinear stress levels.

Unlike the linear analysis, the maximum strength analysis is based upon the concept of bending and buckling of cylinders with both large-deflection stress redistributions and localized nonlinear stress-strain behavior occurring prior to and during the buckling process. This behavior appears to be more representative of the failure mechanism in compressed shells and, at least from the limited study results reflected in Table I, it shows that there is a strong question of conservatism in a common design procedure of the type recommended in Reference 9. The conservatism will be amplified by considerations of imperfections, since the 0.75 "knockdown" factor has been difficult to justify by the maximum strength approach. Of course, for designs operating in the linear elastic range, for designs with light stiffening, and for designs in which local buckling is permitted to occur before general buckling, the conservative approach may be justified. However, the discussion here concerns modern aircraft applications and, thus, the type of structure implied is that described by closely spaced, moderately heavy stiffening which neither yields at

limit load, buckles locally prior to general buckling, nor fails in catastrophic fashion.

From Table I and Figure 1, it can be seen that with a yield stress of about 48 ksi for 2024-T3 aluminum alloy, the combination of 60 stringers and 39 rings with slightly increased basic shell-wall thickness is a great deal more efficient than a 60-stringer cylinder reflecting heavier stringers and a lighter basic skin. The result is consistent with previous findings based on purely linear elastic theory (see, for example, Reference 16) that, for a given set of cylinder properties, external stringers and external rings are the most efficient combination for compressive loading cases. Also, in Reference 40, Meller and Mayers, on the basis of results of a linear elastic, large-deflection analysis of imperfect cylinders, show the importance of wavelength control in the snapthrough buckling of unstiffened compressed shells and the beneficial role that circumferential stiffening can play with respect to critical wavelengths and, in turn, buckling strength. As mentioned earlier, the postbuckled state of failed shells is important; whereas catastrophic collapse is typical of unstiffened thin cylinders under compression, the postbuckled state would appear to be less severe when closely spaced ring stiffening is used in combination with stringer stiffening. Photographs of buckled unstiffened, stringer-stiffened and ring-stiffened, and ring- and stringer-stiffened shells are presented in References 46, 32, and 47, respectively. As a point of interest, in Reference 32 it is mentioned that "the lightly ring-stiffened and the stringer-stiffened shells all buckled with a loud snap whereas the heavily ring-stiffened shells exhibited a more gentle type of buckling". Unfortunately, according to Peterson,[1] there is no test data in existence for buckling under compressive loadings of stringer- and ring-stiffened shells in which local buckling does not precede general instability. Further, according to Peterson again,[1] testing through 1969 has not disclosed any type of stiffened cylinder construction that fails in general instability under compression and is immune to low failing loads. Perhaps the use of "effectively thick" stiffened cylinders and maximum strength theory can be useful in

assisting in the resolution of this very practical design optimization problem.

Credibility of Maximum Strength Analysis

For practical shells of closely stiffened or sandwich construction under compressive loading, the effective radius-to-thickness ratio lies between 100 and 300. Below 100, plastic buckling (with yielding) is involved and is of little interest to the aircraft shell design problem. Above about 300, the effects of initial imperfections and local buckling lower the general buckling strength in increasingly deleterious fashion and, hence, exact too great a weight penalty from the basic load-carrying structure; this weight penalty, in turn, is amplified through the overall vehicle. The critical situation being faced with regard to basic structural weight is evidenced by the continued reference for at least a decade to advanced composite materials as the panacea for the structural efficiency problem.

For the "effectively thick" cylinders in the effective radius-to-thickness range 100-300, the imperfections tend to minimize their influence and the failure mechanism involves both the inherent sensitivity of thin shells under compression to initial imperfections and the nonlinear behavior of the material (see, for example, Hutchinson and Koiter[6] and Mayers and Wesenberg[10,11]). This behavior is quite different from that of flat rectangular plates under compression where the failure mechanism depends on the phenomenon of buckle wavelength change and the nonlinear action of the material (see References 48 and 43); imperfection sensitivity, which is important in the bifurcation region, has little effect on the maximum strength of postbuckled plates. In "effectively thick" shells, even with small imperfections present, bending and buckling in a nonlinear-elastic sense occur prior to and at maximum load. Thus, neither plastic buckling of thick shells nor elastic buckling of very thin shells is a physically valid approach for "effectively thick" shells, the generous use of plasticity correction factors and initial imperfection "knockdown" factors notwithstanding. The state of the art

is assessed very succinctly by Almroth et al.[2] in the statement, "Although it is felt that the method recommended here represents a clear advantage over present design practices, it is still an interim solution acceptable only because totally satisfactory methods are not available".

For "effectively thick" cylinders, the discrepancy between experiment and theory can be as much as 40%. This, of course, is far less discrepancy than that found with unstiffened cylinders where the experimental results may be 80% lower than the theoretical predictions. With a reduction factor of 0.75 recommended in, say, Reference 9 for shells with closely spaced, moderately heavy stiffening, and for the effective radius-to-thickness ratio range 100-300, it is reasonable to assume that both imperfections and material nonlinearity affect the failure load in a maximum strength sense as opposed to the concept[9] of perfect-shell bifurcation buckling with applications of semiempirical correction factors for imperfection sensitivity and material nonlinearity. The relatively new design procedure of Reference 2, which includes the Koiter theory as one of its bases, is restricted to linear material behavior.

Although Mayers and Wesenberg[10,11] have demonstrated the combined effects of imperfections and material nonlinearity on shell maximum strength, no other attempt has been made to offer a possible reason other than imperfections for the large scatter appearing in plots of myriad nondimensionalized experimental buckling stress results versus radius-to-thickness ratio (see, for example, References 25 and 46). Donnell,[13] in an amazing effort as far back as 1934, attempted, among other things, to correlate the buckling strengths of unstiffened, imperfect steel, brass, and Dural cylinders with a semiempirical criterion based upon material yielding of buckled sheet; he achieved good success in the radius-to-thickness range 150-1500. Since the Donnell theoretical developments were not rigorous, it is a source of bewilderment as to the lack of interest shown in Donnell's intuitive reasoning and results in the years following when so much effort was expended in attacking

the thin shell, axial compression buckling problem and attempting to explain both qualitatively and quantitatively the discrepancy between experiment and theory.

In 1965, Weingarten et al.[25] proposed a design formula for the buckling of axially compressed shells based upon assessment of their own and the experimental results of many other investigators. The formula recognized the dependence of buckling load reduction on the radius-to-thickness ratio and, in essence, formed the lower bound to data exhibiting a very large scatter band. The Weingarten et al. formula appears in Appendix II. On the hypothesis that some of the scatter in test results can be attributed to nonlinear material behavior during the buckling process, a major modification of the Weingarten et al. formula is made in Appendix II to cover the scatter band obtained from the experimental data presented in References 25 and 46 in the form of nondimensional buckling stress parameter versus radius-to-thickness ratio. The scatter band limits for the combined data are shown in Figure 3. The lower-bound curve, which is slightly lower than that of Weingarten et al., corresponds approximately to materials with a proportional limit strain of 0.001, whereas the upper-bound curve corresponds to materials with a proportional-limit strain of about 0.007. Interestingly, aircraft metals reflect this range of values for proportional-limit strain at room temperature. Some of the steels are on the lower bound; a material such as titanium lies on the upper bound. The trend of the curves bears out the trend obtained by Donnell[13] for his own tests with brass and steel cylinders and for those of Lundquist[14] with Dural. For a perfect cylinder, the classical buckling strain is inversely proportional to the radius-to-thickness ratio; thus, as shown in Figure 3, in the lower radius-to-thickness ratio range especially, the scatter band can be traversed for a constant value of radius-to-thickness ratio by designating materials in increasing values of their proportional-limit strains. This implies that a perfect cylinder with a material proportional-limit strain of 0.001 remains linear elastic only at a radius-to-thickness ratio above 600, whereas a material with a proportional-limit strain of 0.006 remains

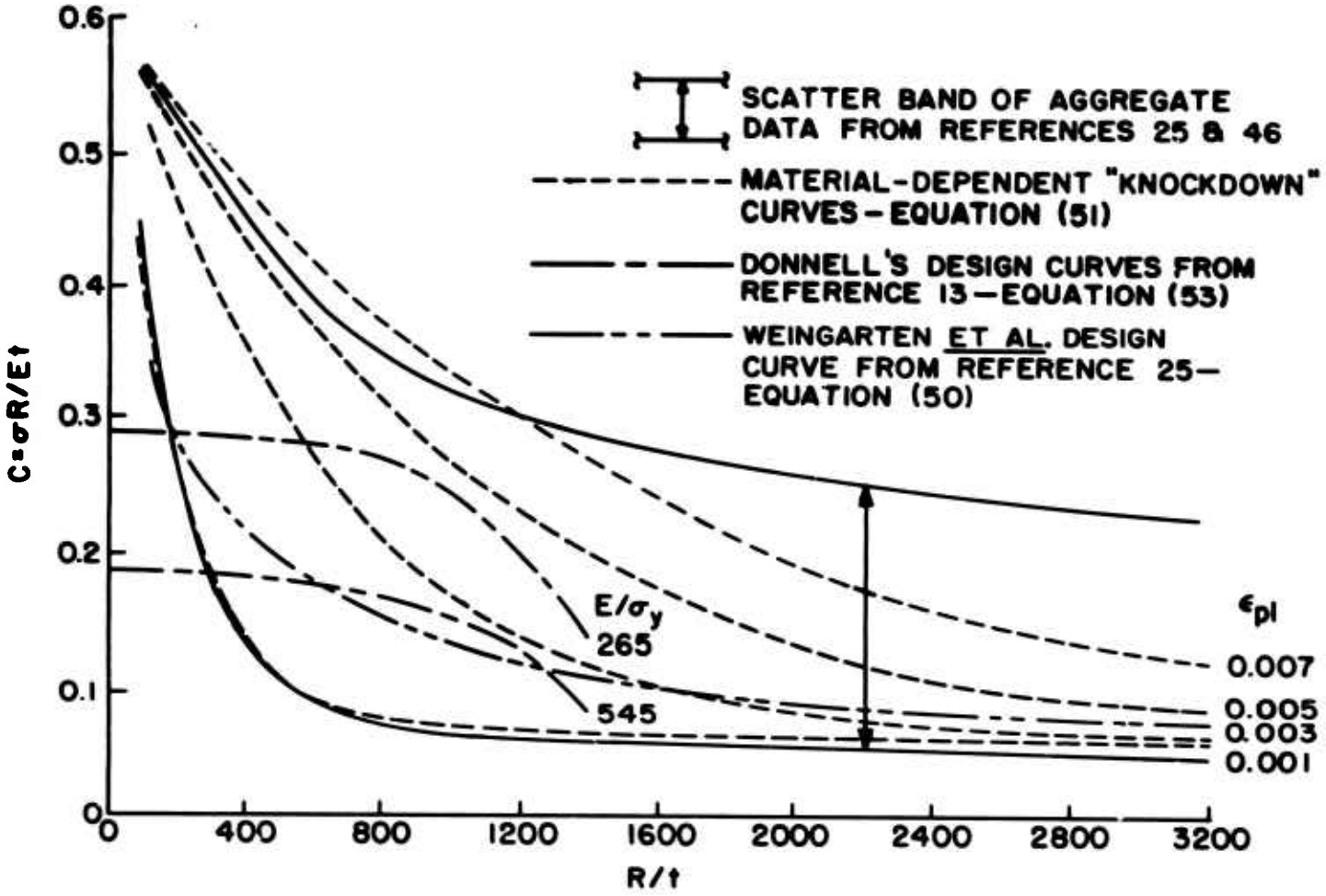

Figure 3. Correlation of Material-Dependent Semiempirical Relation of Appendix II With Scatter Band for Experimental Axial Compression Buckling Stress Coefficients.

linear elastic above a radius-to-thickness ratio of 100. Naturally, actual cylinders are not perfect; therefore, bending and buckling in a nonlinear-elastic sense take place with imperfections and nonlinear material behavior both contributing to the failure mechanism in imperfect shells. The difference in material stress-strain curves must manifest itself and contribute to the scatter in test results. This conclusion is consistent with the maximum strength results obtained by Mayers and Wesenberg in References 10 and 11 for materials such as electroformed copper and nickel, aluminum, and stainless steel.

Another test of the credibility of the maximum strength approach is available through the experimental work of Weller et al. on longitudinally stiffened steel cylinders.[12] In a series of 88 tests conducted on 5- and 7-in.-radius shells with essentially the same effective thicknesses in the stiffening direction, the investigators obtained the rather anomalous result that on the average the thinner (14-in.) cylinders were stronger in buckling than the thicker (10-in.) cylinders when the experimental buckling stresses were ratioed to the buckling stresses predicted by the classical, eccentrically stiffened, orthotropic shell theory.[15,16] The buckling-stress ratios as well as other pertinent details are given in Table II for 4 of the 12 cylinders in Reference 12 having length-to-radius ratios equal to or greater than unity; the cylinder designations are those of Reference 12. Also included in Table II are the buckling-stress ratios based upon the theoretical predictions of the present maximum strength theory for the 4 cylinders using the actual stress-strain curves for the materials involved shown in Figure 4. Although the steel materials used in the tests exhibit the identical Young's modulus, the nonlinear portions of the curves are significantly different. With the weaker material assigned to the 5-in. radius cylinders, the results as presented in Reference 12 tend to contradict all previous experience. However, in the light of the corrected buckling-stress ratios given in Table II for the subject cylinders, it can be seen that the two 7-in.-radius cylinders retain the same stress ratios (the behavior is truly linear elastic) whereas marked changes occur in

TABLE II. COMPARISON OF EXPERIMENTAL BUCKLING STRESS COEFFICIENTS BASED ON CLASSICAL AND MAXIMUM STRENGTH THEORIES

CYLINDER NO. (REFERENCE 12)	R (in.)	t (in.)	A_s/dt	I_s/dt^3	$\bar{t}_x$ (in.)	$R/\bar{t}_x$	σ_e (ksi)	$(\sigma_e/\sigma_{cr})^*$	$(\sigma_e/\sigma_{max})^{**}$
SZ-3	5.02	0.0120	0.174	0.0143	0.0141	358	39.5	0.672	0.789
7-L	5.02	0.0112	0.198	0.0210	0.0135	372	37.2	0.699	0.855
13-L	6.90	0.0115	0.387	0.0628	0.0160	432	26.2	0.901	0.901
24-L	6.92	0.0105	0.226	0.0340	0.0129	536	24.6	0.756	0.756

*σ_{cr} based on Baruch/Singer-NASA buckling criterion for linear elastic, perfect cylinders (see References 15 and 16); (σ_e/σ_{cr}) taken from Reference 12.

**σ_{max} based on maximum strength analysis outlined in Appendix I and developed in References 10 and 11. To approximate perfect shells, the imperfection amplitude $\xi 11_0$ is taken equal to 0.0001 . Stress-strain curve parameters E , K , and N are given in Figure 4 for the test materials.

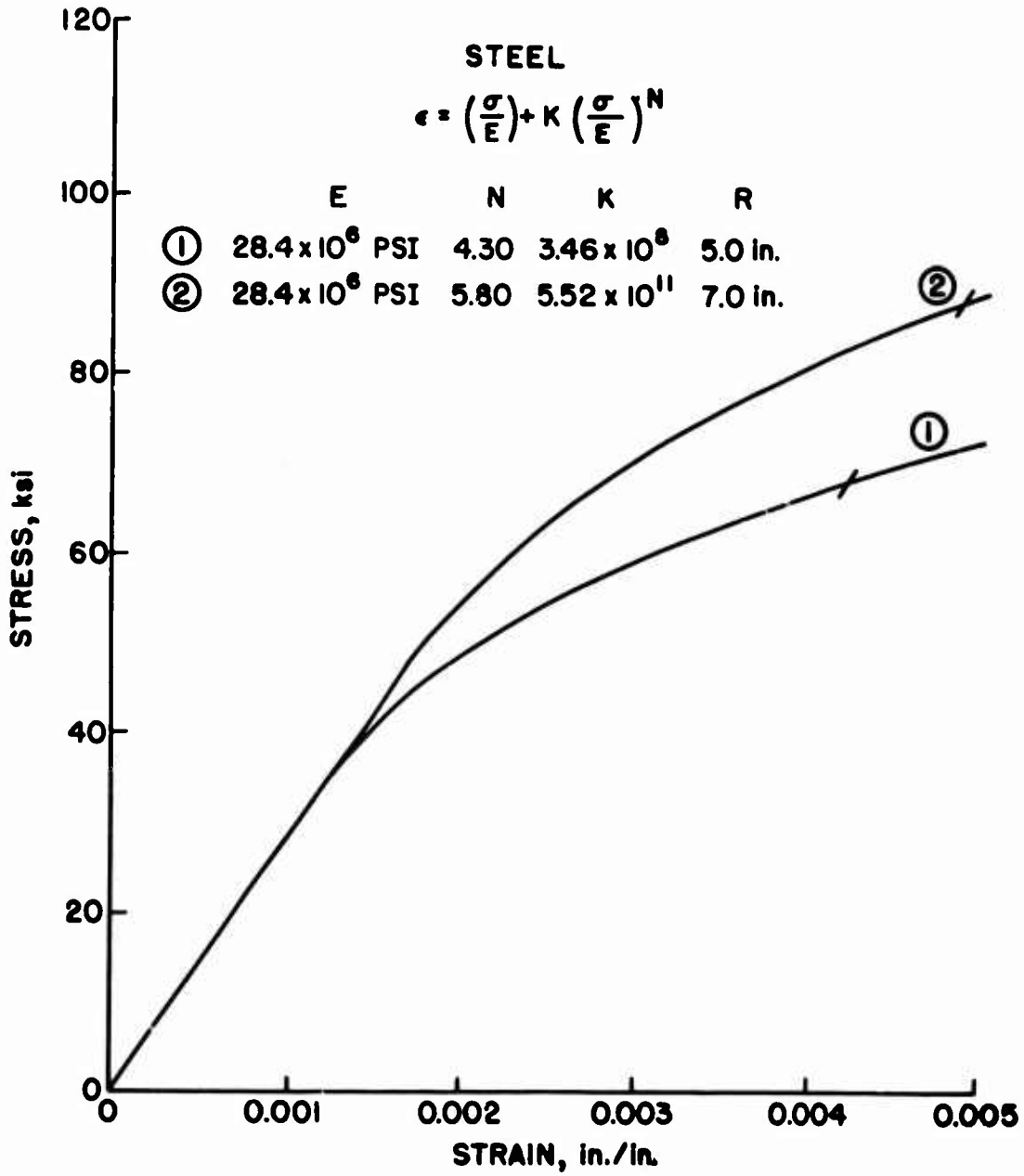

Figure 4. Stress-Strain Curves for Steel Cylinders of Reference 12.

the stress ratios for the 5-in.-radius cylinders due to very definite inelastic behavior. Indeed, 10-in. cylinders SZ-3 and 7-L reverse the anomalous trend appearing in Reference 12 with respect to 14-in. cylinder 24-L; however, although the gap is closed significantly with respect to cylinder 13-L, the very heavy stiffening of the latter relative to that of SZ-3 and 7-L (see Table II) prevents an actual reversal of the trend. Had the assignment of material to the 10- and 14-in. cylinders been reversed prior to fabrication, the 14-in. cylinders would have appeared to be much weaker on the average than the 10-in. cylinders. The tendency then, no doubt, would have been to attribute the discrepancy entirely to imperfection sensitivity of the "effectively thinner" 14-in. cylinders. Another point of interest is that the question of yielding of the material in the 5-in.-radius cylinders is not involved. The average compressive stresses are well below the 0.2% offset yield stress of the material for the 5-in.-radius cylinders. The maximum local stresses at buckling are somewhat higher, although still below the yield stress. Postbuckling local maximum stresses are another problem when catastrophic snapthrough occurs; such considerations are beyond the scope of the present discussion. However, they are discussed in Reference 36.

The discussion and results presented in this section are believed to lend credence to the concept of a maximum strength analysis of compressed cylinders. The results are consistent with the conclusions of Mayers and Wesenberg[10,11] that the effects of material nonlinearity together with those of initial imperfections control the buckling strength of compressed cylinders. Material nonlinearity plays the more significant role quantitatively for "effectively thick" cylinders (closely stiffened and sandwich construction), especially when the material exhibits a large ratio of yield stress to proportional limit stress (or a low value of the exponent appearing in the Ramberg-Osgood[38] representation for uniaxial stress-strain curves of conventional aircraft metals).

The experimental results of Weller et al. in Reference 12 when interpreted in the light of the maximum strength concept of compressed cylinder failure advanced in References 10 and 11 as well as in the present effort demonstrate the sensitivity of the buckling process to both material nonlinearity and initial imperfections. The former phenomenon is vividly illustrated for the two 5-in.-radius cylinders taken from Reference 12 by noting the experimental buckling stress levels given in Table II with respect to the stress-strain curves of Figure 4. Offhand, it would appear that the buckling stresses (or average axial stresses at buckling) carried by the 10-in. cylinders are essentially in the linear elastic range. However, the maximum strength analysis for imperfect shells involves both bending and buckling (rather than the classical concept of bifurcation from a perfect shell membrane state of uniform stress) so that local effective stress levels (membrane plus bending) can be well into the nonlinear range of the stress-strain curve. Failure is an integrated effect for the shell buckling problem; thus, buckling based on the maximum strength analysis for the 10-in. cylinders, although outwardly appearing to be essentially linear elastic, actually is significantly inelastic. It is obvious that the 14-in. cylinders remain linear elastic during the bending and buckling process because of the lower stress levels involved and the increased linear portion of the material stress-strain curve for these cylinders. One more point of note is that the nonlinear material behavior begins to make its influence felt in the vicinity of the proportional limit. The fact that average stress levels may be well below the 0.2% offset yield stress for a material does not justify treating the buckling problem on the basis of linear elastic material behavior up to the yield point stress level. The assumption of a perfectly elasto-plastic material (with or without strain hardening) is a case in point. Obviously there is more to the perplexing behavior of axially compressed thin shells than, for example, the effects of imperfection sensitivity, prebuckling deformations, and boundary conditions. It is felt that more attention will have to be given to material nonlinearity effects, especially if

the optimization with respect to weight and cost of stiffness-critical shell structures is to become a reality for conventional, sandwich, and advanced composite materials at both room and elevated temperatures.

CONCLUDING REMARKS

A maximum strength analysis of initially imperfect, axially compressed, eccentrically stiffened cylinders based upon a modification of Reissner's variational principle, von Kármán-Donnell shell theory, and a deformation theory of plasticity is undertaken to optimize in gross fashion a 2024-T3 aluminum alloy configuration subject to the condition that no yielding take place in the design sense. The results are compared with the predictions of linear theory for perfect shells with applied buckling load reduction factors to account for imperfections and inelastic behavior. For the optimized cylinder, combining stringer- and ring-stiffening, the maximum strength analysis is shown to be less conservative.

To lend credence to the maximum strength approach, the technique is used to correlate the results obtained for several 10- and 14-in. diameter cylinders constructed of steel with different proportional limits, respectively. The maximum strength results explain the apparently anomalous behavior displayed by the two sets of cylinders when the experimental buckling stresses are ratioed to the elastic theory predictions of classical theory for eccentric stiffening. It is demonstrated that material nonlinearity is an important factor in buckling load calculations of imperfect shells at average compressive stresses well below the material yield stress, especially in materials exhibiting lower exponents in the Ramberg-Osgood representation of the uniaxial stress-strain curve for aircraft metals. This factor is of consequence for materials at elevated temperatures and for composites using high-strength filaments such as boron.

The effect of material nonlinearity in the effective radius-to-thickness range characterizing closely spaced, moderately heavy stiffened and sandwich shells suggests that it may serve to explain some of the large scatter appearing in experimental data which is presently attributed mainly to initial imperfections. A simple, material-dependent relation for buckling coefficients is offered to show that the scatter band encompassing myriad test results can be spanned at any radius-to-thickness ratio below 1500

as a function of proportional-limit strains in the range 0.001 through 0.007. Interestingly, this range covers the proportional limit strains for conventional metals. The qualitative sensitivity of the buckling coefficient relationship to material nonlinearity cannot be overlooked when attempting to explain the discrepancy between test and theory for axially compressed shells in the "effectively thick" range (practical stiffened and sandwich shells). The work of Donnell in 1934 in this respect, although open to question with regard to rigor of analysis and adopted failure criterion, was apparently too soon overlooked in the massive theoretical attack on the small and large deflection stability problems of perfectly elastic cylinders which has taken place in the past 30 years.

In view of the desire for increased structural efficiency, the concept of bending and buckling in the inelastic range well below the 0.2% offset yield stress should be given some consideration for failure load determination when "effectively thick" shells (closely spaced, moderately heavy stiffening and sandwich cylinders) are involved. Optimized stringer- and ring-stiffened shells should not exhibit catastrophic snapthrough collapse at limit load in the sense associated with very thin, unstiffened cylinders. Further, local buckling of the skin between stiffening elements should not occur prior to general buckling. Unfortunately, there is no test data for stringer- and ring-stiffened shells in which there is an absence of a large discrepancy between theory and experiment; thus, this gap in experimental data should be closed. Apparently, the effect of local skin buckling prior to general buckling reduces stiffness for the latter more than would be desired in efficient design. Additionally, there is strong evidence in the present work to suggest that the axial compression test data scatter, presently attributed mainly to initial imperfections, may be appreciably sensitive to material nonlinearity at buckling in the radius-to-thickness range of practical interest. A modest experimental program is recommended for constant radius-to-thickness ratio cylinders of several materials exhibiting proportional limit strains from 0.001 (steel) to 0.007 (titanium) wherein the

fabrication process is identical. In this manner, some assessment of the magnitude of scatter due to material nonlinearity effects can be obtained, other than that implied from the stringer-stiffened-cylinder test program of Reference 12 and the presentation contained in Appendix II.

LITERATURE CITED

1. Peterson, J. P., BUCKLING OF STIFFENED CYLINDERS IN AXIAL COMPRESSION AND BENDING – A REVIEW OF TEST DATA, NASA Technical Note D-5561, National Aeronautics and Space Administration, 1969.

2. Almroth, B. O., Burns, A. B., and Pittner, E. V., DESIGN CRITERIA FOR AXIALLY LOADED CYLINDRICAL SHELLS, AIAA Journal, Vol. 7, No. 6, June 1970, pp. 714-720.

3. Hoff, N. J., THE PERPLEXING BEHAVIOR OF THIN CIRCULAR CYLINDRICAL SHELLS IN AXIAL COMPRESSION, Israel Journal of Technology, Vol. 24, No. 1, 1966, pp. 1-28.

4. Hoff, N. J., THIN SHELLS IN AEROSPACE STRUCTURES, Astronautics and Aeronautics, Vol. 5, No. 2, February 1967, pp. 26-45.

5. Stein, M., RECENT ADVANCES IN THE INVESTIGATION OF SHELL BUCKLING, AIAA Journal, Vol. 6, No. 12, December 1968, pp. 2339-2345.

6. Hutchinson, J. W., and Koiter, W. T., POSTBUCKLING THEORY, Applied Mechanics Reviews, Vol. 23, No. 12, December 1970, pp. 1353-1366.

7. Baker, E. H., Capelli, A. P., Kovalevsky, L., Rish, F. L., and Verette, R. M., SHELL ANALYSIS MANUAL, North American Aviation, Inc. (for National Aeronautics and Space Administration) Report N68-2482, April 1968.

8. Smith, G. W., Spier, E. E., et al., THE STABILITY OF ECCENTRICALLY STIFFENED CIRCULAR CYLINDERS, Vols. I-VI, Convair Division of General Dynamics (for National Aeronautics and Space Administration) Report GDC DDG 67-006, June 1967.

9. Anon., BUCKLING OF THIN-WALLED CIRCULAR CYLINDERS, National Aeronautics and Space Administration SP-8007, August 1968.

10. Mayers, J., and Wesenberg, D. L., THE MAXIMUM STRENGTH OF INITIALLY IMPERFECT, AXIALLY COMPRESSED, CIRCULAR CYLINDRICAL SHELLS, Stanford University; USAAVLABS Technical Report 69-60, U.S. Army Aviation Materiel Laboratories, Fort Eustis, Virginia, August 1969, AD862102.

11. Wesenberg, D. L., and Mayers, J., FAILURE ANALYSIS OF INITIALLY IMPERFECT, AXIALLY COMPRESSED, ORTHOTROPIC, SANDWICH AND ECCENTRICALLY STIFFENED, CIRCULAR CYLINDRICAL SHELLS, Stanford University; USAAVLABS Technical Report 69-86, U.S. Army Aviation Materiel Laboratories, Fort Eustis, Virginia, December 1969, AD866199.

12. Weller, T., Singer, J., and Nachmani, S., RECENT EXPERIMENTAL STUDIES ON THE BUCKLING OF INTEGRALLY STRINGER-STIFFENED CYLINDRICAL SHELLS, Technion – Israel Institute of Technology; TAE Report 100, April, 1970.

13. Donnell, L. H., A NEW THEORY FOR THE BUCKLING OF THIN CYLINDERS UNDER AXIAL COMPRESSION AND BENDING, Transactions of the AMSE, Vol. 56, 1934, pp. 795-806.

14. Lundquist, E. E., STRENGTH TESTS OF THIN-WALLED DURALUMINUM CYLINDERS IN COMPRESSION, National Advisory Committee for Aeronautics, NACA Technical Report 473, 1933.

15. Baruch, M., and Singer, J., EFFECT OF ECCENTRICITY OF STIFFENERS ON THE GENERAL INSTABILITY OF STIFFENED CYLINDRICAL SHELLS UNDER HYDROSTATIC PRESSURE, Journal of Mechanical Engineering Sciences, Vol. 5, No. 1, 1963, pp. 23-27.

16. Block, D. L., Card, M. F., and Mikulas, M. M., Jr., BUCKLING OF ECCENTRICALLY STIFFENED ORTHOTROPIC CYLINDERS, National Aeronautics and Space Administration, NASA Technical Note D-2960, 1965.

17. Stein, M., and Mayers, J., COMPRESSIVE BUCKLING OF SIMPLY SUPPORTED CURVED PLATES AND CYLINDERS OF SANDWICH CONSTRUCTION, National Advisory Committee for Aeronautics, NACA Technical Note 2601, 1952.

18. Lorenz, R., ACHSENSYMMETRISCHE VERZERRUNGEN IN DÜNNWANDIGEN HOHLZYLINDERN, Zeitschrift des Vereines Deutscher Ingenieure, Vol. 52, p. 1707, 1908.

19. Timoshenko, S., EINIGE STABILITÄTSPROBLEME ELASTIZITÄTSTHEORIE, Zeitschrift für Mathematik und Physik, Vol. 58, p. 337, 1910.

20. Southwell, R. V., ON THE GENERAL THEORY OF ELASTIC STABILITY, Philosophical Transactions of the Royal Society of London, Series A, Vol. 213, p. 187, 1914.

21. Babcock, C. D., Jr., and Sechler, E. E., THE EFFECT OF INITIAL IMPERFECTIONS ON THE BUCKLING STRESS OF CYLINDRICAL SHELLS, National Aeronautics and Space Administration, NASA Technical Note D-2005, 1963.

22. Almroth, B. O., Holmes, A. M. C., and Brush, D. O., AN EXPERIMENTAL STUDY OF THE BUCKLING OF CYLINDERS UNDER AXIAL COMPRESSION, Experimental Mechanics, Vol. 4, 1963, p. 263.

23. Horton, W. H., and Durham, S. C., IMPERFECTIONS, A MAIN CONTRIBUTOR TO SCATTER IN EXPERIMENTAL VALUES OF BUCKLING LOAD, International Journal of Solids and Structures, Vol. 1, 1959, p. 59.

24. Tennyson, R. C., BUCKLING OF CIRCULAR CYLINDRICAL SHELLS IN AXIAL COMPRESSION, AIAA Journal, Vol. 2, No. 7, 1964, pp. 1351-1353.

25. Weingarten, V. I., Morgan, E. J., and Seide, P., ELASTIC STABILITY OF THIN-WALLED CYLINDRICAL AND CONICAL SHELLS UNDER AXIAL COMPRESSION, AIAA Journal, Vol. 3, No. 3, 1965, pp. 500-505.

26. Koiter, W. T., OVER DE STABLITEIT VAN HETELASTISCH EVENWICHT, Thesis, Delft, H. J. Paris, Amsterdam, 1945. English Translation Issued as U.S. Air Force Flight Dynamics Laboratory Technical Report 70-25, February 1970.

27. Koiter, W. T., THE EFFECT OF AXISYMMETRIC IMPERFECTIONS ON THE BUCKLING OF CYLINDRICAL SHELLS UNDER AXIAL COMPRESSION, Lockheed Missiles and Space Company, Report 6-90-63-86, August 1963.

28. Brush, D. O., IMPERFECTION SENSITIVITY OF STRINGER STIFFENED CYLINDERS, AIAA Journal, Vol. 6, No. 12, December 1968, pp. 2445-2447.

29. Madsen, W. A., and Hoff, N. J., THE SNAP-THROUGH AND POSTBUCKLING EQUILIBRIUM BEHAVIOR OF CIRCULAR CYLINDRICAL SHELLS UNDER AXIAL LOAD, Stanford University; SUDAER No. 227, April 1965.

30. Singer, J., Baruch, M., and Harari, O., ON THE STABILITY OF ECCENTRICALLY STIFFENED CYLINDRICAL SHELLS UNDER AXIAL COMPRESSION, International Journal of Solids and Structures, Vol. 3, No. 4, July 1967, pp. 445-470.

31. Singer, J., THE INFLUENCE OF STIFFENER GEOMETRY AND SPACING ON THE BUCKLING OF AXIALLY COMPRESSED CYLINDRICAL AND CONICAL SHELLS, Technion – Israel Institute of Technology; TAE Report 68, October 1967.

32. Singer, J., Arbocz, J., and Babcock, C. D., Jr., BUCKLING OF IMPERFECT STIFFENED CYLINDRICAL SHELLS UNDER AXIAL COMPRESSION, AIAA Journal, Vol. 9, No. 1, January 1971, pp. 68-75.

33. Batterman, S. C., PLASTIC BUCKLING OF AXIALLY COMPRESSED CYLINDRICAL SHELLS, AIAA Journal, Vol. 3, No. 2, February 1965, pp. 316-325.

34. Hutchinson, J. W., ON THE POSTBUCKLING BEHAVIOR OF IMPERFECTION-SENSITIVE STRUCTURES IN THE PLASTIC RANGE, Harvard University; Report SM-41, July 1970.

35. von Kármán, T., and Tsien, H. S., THE BUCKLING OF THIN CYLINDRICAL SHELLS UNDER AXIAL COMPRESSION, Journal of the Aeronautical Sciences, Vol. 8, No. 8, June 1941, pp. 303-312.

36. Mayers, J., and Rehfield, L. W., FURTHER NONLINEAR CONSIDERATIONS IN THE BUCKLING OF AXIALLY COMPRESSED CIRCULAR CYLINDRICAL SHELLS, Stanford University; SUDAER 197, June 1964. Also DEVELOPMENTS IN MECHANICS, Vol. 3, Part 1, New York, John Wiley and Sons, Inc., 1967, pp. 145-160.

37. Hoff, N. J., Madsen, W. A., and Mayers, J., THE POSTBUCKLING EQUILIBRIUM OF AXIALLY COMPRESSED CIRCULAR CYLINDRICAL SHELLS, AIAA Journal, Vol. 4, No. 1, January 1966, pp. 126-133.

38. Ramberg, W., and Osgood, W. R., DESCRIPTION OF STRESS-STRAIN CURVES BY THREE PARAMETERS, National Advisory Committee for Aeronautics, NACA Technical Note 902, 1943.

39. Gerard, G., COMPRESSIVE AND TORSIONAL BUCKLING OF THIN-WALLED CYLINDERS IN YIELD REGION, National Advisory Committee for Aeronautics, NACA Technical Note 3726, 1956.

40. Meller, E., and Mayers, J., ON THE OPTIMUM PROPORTIONING OF STIFFENED CIRCULAR CURVED PLATES AND SHELLS FOR AXIAL COMPRESSION LOADING, USAAVLABS Technical Report 70-9, U.S. Army Aviation Materiel Laboratories, Fort Eustis, Virginia, March 1970, AD871425.

41. Mayers, J., and Budiansky, B., ANALYSIS OF BEHAVIOR OF SIMPLY SUPPORTED FLAT PLATES COMPRESSED BEYOND BUCKLING INTO THE PLASTIC RANGE, National Advisory Committee for Aeronautics, NACA Technical Note 3368, 1955.

42. Mayers, J., Nelson, E., and Smith, L. B., MAXIMUM STRENGTH ANALYSIS OF POSTBUCKLED RECTANGULAR PLATES, Stanford University; SUDAAR 215, December 1964.

43. Mayers, J., and Nelson, E., ELASTIC AND MAXIMUM STRENGTH ANALYSES OF POSTBUCKLED RECTANGULAR PLATES BASED UPON MODIFIED VERSIONS OF REISSNER'S VARIATIONAL PRINCIPLE, Presented at AIAA Sixth Aerospace Sciences Meeting, AIAA Paper No. 68-171, New York, January 1968. Also USAAVLABS Technical Report 69-64, U.S. Army Aviation Materiel Laboratories, Fort Eustis, Virginia, July 1970, AD872821.

44. Timoshenko, S., THEORY OF ELASTIC STABILITY, New York, McGraw-Hill Book Co., Inc., 1936, p. 396.

45. Card, M. F., and Jones, R. M., EXPERIMENTAL AND THEORETICAL RESULTS FOR BUCKLING OF ECCENTRICALLY STIFFENED CYLINDERS, National Aeronautics and Space Administration, NASA Technical Note D-3639, October 1966.

46. Harris, L. A., Suer, H. S., Skene, W. T., and Benjamin, R. J., THE STABILITY OF THIN-WALLED UNSTIFFENED CIRCULAR CYLINDERS UNDER AXIAL COMPRESSION INCLUDING THE EFFECTS OF INTERNAL PRESSURE, Journal of the Aeronautical Sciences, Vol. 24, No. 8, August 1957, pp. 587-596.

47. Card, M. F., BENDING TESTS OF LARGE-DIAMETER STIFFENED CYLINDERS SUSCEPTIBLE TO GENERAL INSTABILITY, National Aeronautics and Space Administration, NASA Technical Note D-2200, April 1964.

48. Stein, M., LOADS AND DEFORMATIONS OF BUCKLED RECTANGULAR PLATES, National Aeronautics and Space Administration, NASA Technical Report R-40, 1959.

APPENDIX I

FOUNDATION OF MAXIMUM STRENGTH ANALYSIS FOR INITIALLY IMPERFECT, ECCENTRICALLY STIFFENED, CIRCULAR CYLINDRICAL SHELLS UNDER AXIAL COMPRESSION

For completeness, the cylindrical shell maximum strength analysis developed in Reference 10 and extended in Reference 11 is presented here in concise form. It is based upon the use of a modified version of the Reissner variational principle, the von Kármán-Donnell strain-displacement relations, and a deformation theory of plasticity. Because the deflections and rotations at maximum load are sufficiently small, as determined by Mayers and Wesenberg in Reference 10, the use of the von Kármán-Donnell theory is justified. The effects of unloading can be neglected;[10,11] hence, the analysis reduces to one of nonlinear elasticity. To avoid the complexity of integrating nonlinear stress distributions through the thickness, a two-element cross section with an intermediate core rigid in shear is used to replace that of the stiffened shell (see Figure 5). The stiffening elements are sufficiently closely spaced so that they may be considered smeared over the shell surface, thus giving rise in the model to implied facing separations h_x , h_y , and h_{xy} . The eccentricty effects of any stiffening elements are accounted for approximately in further definitions of the quantities h_x , h_y , and h_{xy} .

The Reissner functional for the orthotropic cylinder model under controlled end shortening, modified to include incompressible plasticity of the material (all Poisson ratios are taken equal to $\frac{1}{2}$), is

$$U'' = 2Et_f \int_0^L \int_0^{2\pi R} \left[\left(\frac{\sigma'_x}{E}\right) \epsilon'_x + \left(\frac{\sigma'_y}{E}\right) \epsilon'_y + \left(\frac{\tau'_{xy}}{E}\right) \gamma'_{xy} + \left(\frac{\sigma''_x}{E}\right) \epsilon''_x \right.$$

$$\left. + \left(\frac{\sigma''_y}{E}\right) \epsilon''_y + \left(\frac{\tau''_{xy}}{E}\right) \gamma''_{xy} - \frac{1}{2} \left[E_1^2 \left(\frac{\sigma'_x}{E}\right)^2 + E_2^2 \left(\frac{\sigma'_y}{E}\right)^2 \right. \right.$$

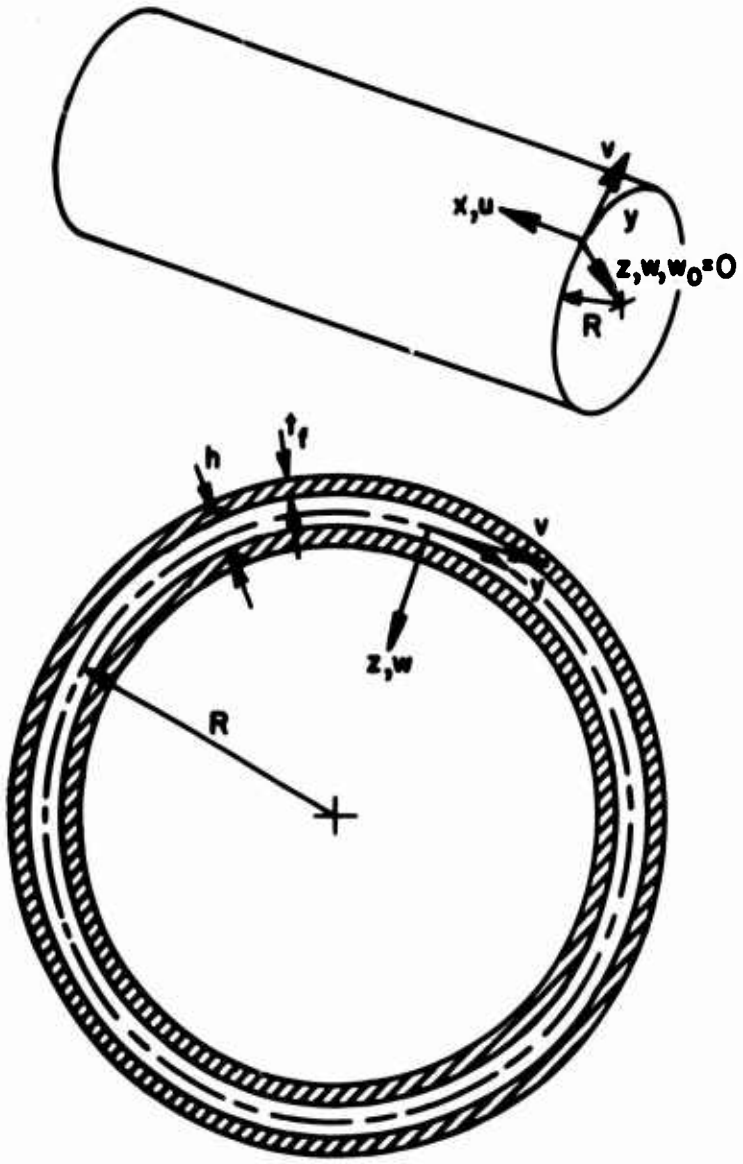

Figure 5. Circular Cylindrical Shell With Two-Element Cross Section.

$$- E_4^2 \left(\frac{\sigma'_x}{E}\right)\left(\frac{\sigma'_y}{E}\right) + 3E_3^2 \left(\frac{\tau'_{xy}}{E}\right)^2 + D_1^2 \left(\frac{\sigma''_x}{E}\right)^2 + D_2^2 \left(\frac{\sigma''_y}{E}\right)^2$$

$$- D_4^2 \left(\frac{\sigma''_x}{E}\right)\left(\frac{\sigma''_y}{E}\right) + 3D_3^2 \left(\frac{\tau''_{xy}}{E}\right)^2 \Bigg]$$

$$- \frac{K}{2(N+1)} \left[\left(\frac{\sigma_{eff}}{E}\right)_t^{N+1} + \left(\frac{\sigma_{eff}}{E}\right)_b^{N+1} \right] \Bigg\} \, dxdy \qquad (1)$$

where

$$\epsilon'_x = u_{,x} + \frac{1}{2} w_{,x}^2 + w_{,x} w_{0,x} \qquad (2)$$

$$\epsilon'_y = v_{,y} + \frac{1}{2} w_{,y}^2 - \frac{w}{R} + w_{,y} w_{0,y} \qquad (3)$$

$$\gamma'_x = u_{,y} + v_{,x} + w_{,x} w_{,y} + w_{0,x} w_{,y} + w_{0,y} w_{,x} \qquad (4)$$

$$\epsilon''_x = \frac{h_x}{2} w_{,xx} \qquad (5)$$

$$\epsilon''_y = \frac{h_y}{2} w_{,yy} \qquad (6)$$

$$\gamma''_{xy} = h_{xy} w_{,xy} \qquad (7)$$

$$\epsilon_{x_{t,b}} = \epsilon'_x \pm \epsilon''_x \qquad (8)$$

$$\epsilon_{y_{t,b}} = \epsilon'_y \pm \epsilon''_y \qquad (9)$$

$$\gamma_{xy_{t,b}} = \gamma'_{xy} \pm \gamma''_{xy} \qquad (10)$$

$$\sigma'_x = (\sigma_{x_t} + \sigma_{x_b})/2 \qquad (11)$$

and

$$\sigma'_y = (\sigma_{y_t} + \sigma_{y_b})/2 \tag{12}$$

$$\tau'_{xy} = (\tau_{xy_t} + \tau_{xy_b})/2 \tag{13}$$

$$\sigma''_x = (\sigma_{x_t} - \sigma_{x_b})/2 = -M_x/h_x t_f \tag{14}$$

$$\sigma''_y = (\sigma_{y_t} - \sigma_{y_b})/2 = -M_y/h_y t_f \tag{15}$$

$$\tau''_{xy} = (\tau_{xy_t} - \tau_{xy_b})/2 = M_{xy}/h_{xy} t_f \tag{16}$$

$$\sigma_{x_{t,b}} = \sigma'_x \pm \sigma''_x \tag{17}$$

$$\sigma_{y_{t,b}} = \sigma'_y \pm \sigma''_y \tag{18}$$

$$\tau_{xy_{t,b}} = \tau'_{xy} \pm \tau''_{xy} \tag{19}$$

$$(\sigma_{eff})^2_{t,b} = (E_1\sigma'_x \pm D_1\sigma''_x)^2 + (E_2\sigma'_y \pm D_2\sigma''_y)^2 - (E_4\sigma'_x \pm D_4\sigma''_x)(E_4\sigma'_y \pm D_4\sigma''_y) + 3(E_3\tau'_{xy} \pm D_3\tau''_{xy})^2 \tag{20}$$

$$E_1^2 = (2t_f E)/E_x \tag{21}$$

$$E_2^2 = (2t_f E)/E_y \tag{22}$$

$$E_3^2 = (2t_f E)/(3G_{xy}) \tag{23}$$

$$E_4^2 = (2t_f E)\left[\mu_x/E_x + \mu_y/E_y\right] = (2t_f E)\left[\frac{\mu_x E_y + \mu_y E_x}{E_x E_y}\right] \tag{24}$$

$$D_1^2 = 1 \tag{25}$$

$$D_2^2 = 1 \tag{26}$$

$$D_3^2 = \frac{2}{3}\,(1 + \nu_x/2 + \nu_y/2) \tag{27}$$

$$D_4^2 = (\nu_y D_x + \nu_x D_y)/\sqrt{D_x D_y} \tag{28}$$

The orthotropic shell constants take the following form for eccentric ring- and stringer-stiffening.

$$\frac{E_x}{2t_f E} = \left(\frac{t}{\bar{t}_x}\right)\frac{[1 + \bar{S} + \bar{R} + \bar{S}\,\bar{R}\,(1-\nu^2)]}{1 + (1-\nu^2)\,\bar{R}} \tag{29}$$

$$\frac{E_y}{2t_f E} = \left(\frac{t}{\bar{t}_x}\right)\frac{[1 + \bar{S} + \bar{R} + \bar{S}\,\bar{R}\,(1-\nu^2)]}{1 + (1-\nu^2)\,\bar{S}} \tag{30}$$

$$\frac{G_{xy}}{2t_f E} = \left(\frac{t}{\bar{t}_x}\right)\frac{[1 + \bar{S} + \bar{R} + \bar{S}\,\bar{R}\,(1-\nu^2)]}{2[1+(1+\nu)(\bar{R}+\bar{S})+\bar{R}\,\bar{S}(1-\nu^2)(1+\nu)]+\mu_y+\mu_x+(1-\nu^2)(\mu_y\bar{S}+\mu_x\bar{R})} \tag{31}$$

and

$$\frac{D_x/2t_f}{(1 - \nu_x\nu_y)} = \frac{Et^3}{12(1-\nu^2)\bar{t}_x}\left[1 + \frac{E_sI_s}{dD}\right] - \bar{C}\,\frac{\bar{S}Et^2(t/\bar{t}_x)}{[1 + (1-\nu^2)\,\bar{S}]}\left(\frac{\bar{z}_s}{R}\right) \qquad (32)$$

$$\frac{D_y/2t_f}{(1 - \nu_x\nu_y)} = \frac{Et^3}{12(1-\nu^2)\bar{t}_x}\left[1 + \frac{E_rI_r}{\ell D}\right] - \bar{C}\,\frac{\bar{R}Et^2(t/\bar{t}_x)}{[1 + (1-\nu^2)\,\bar{R}]}\left(\frac{\bar{z}_r}{R}\right) \qquad (33)$$

$$D_{xy}/2t_f = \frac{Et^3}{12(1-\nu^2)\bar{t}_x}\left[1 - \frac{\nu_x}{2} - \frac{\nu_y}{2} + \frac{1}{2}\left(\frac{G_sJ_s}{dD} + \frac{G_rJ_r}{\ell D}\right)\right.$$

$$\left. - \frac{1}{2}\left(\nu_y\,\frac{E_sI_s}{dD} + \nu_x\,\frac{E_rI_r}{\ell D}\right)\right] + \bar{C}\left\{\frac{\nu_y}{2}\left[\frac{\bar{S}Et^2(t/\bar{t}_x)}{[1 + (1-\nu^2)\,\bar{S}]}\left(\frac{\bar{z}_s}{R}\right)\right]\right.$$

$$+ \frac{\nu_x}{2}\left[\frac{\bar{R}Et^2(t/\bar{t}_x)}{[1 + (1-\nu^2)\,\bar{R}]}\left(\frac{\bar{z}_r}{R}\right)\right]$$

$$\left. - \frac{1}{2}\left[\frac{(1-\nu^2)\,\bar{R}\,\bar{S}Et^2(t/\bar{t}_x)}{2 + 2(1+\nu)(\bar{R}+\bar{S}) + 2\bar{R}\,\bar{S}(1-\nu^2)(1+\nu)}\left(\frac{\bar{z}_s}{R} + \frac{\bar{z}_r}{R}\right)\right]\right\} \qquad (34)$$

$$\left(\frac{h_x}{\bar{t}_x}\right)^2 = \frac{1}{3}\,\frac{(1 - \nu_x\nu_y)}{(1-\nu^2)}\left(\frac{t}{\bar{t}_x}\right)^3\left[1 + \frac{E_sI_s}{dD}\right]$$

$$- \bar{C}\,\frac{4\bar{S}(1 - \nu_x\nu_y)}{[1 + (1-\nu^2)\,\bar{S}]}\left(\frac{t}{\bar{t}_x}\right)^3\left(\frac{\bar{z}_s}{R}\right) \qquad (35)$$

and

$$\left(\frac{h_y}{\bar{t}_x}\right)^2 = \frac{1}{3}\,\frac{(1-\nu_x\nu_y)}{(1-\nu^2)}\left(\frac{t}{\bar{t}_x}\right)^3\left[1+\frac{E_rI_r}{\ell D}\right]$$

$$-\bar{C}\,\frac{4R(1-\nu_x\nu_y)}{[1+(1-\nu^2)\,\bar{R}]}\left(\frac{t}{\bar{t}_x}\right)^3\left(\frac{\bar{z}_r}{R}\right) \qquad (36)$$

$$\left(\frac{h_{xy}}{\bar{t}_x}\right)^2 = \frac{1}{3}\,\frac{[1+(\nu_x/2)+(\nu_y/2)]}{(1-\nu^2)}\left(\frac{t}{\bar{t}_x}\right)^3\left[1-\frac{\nu_x}{2}-\frac{\nu_y}{2}\right.$$

$$\left.+\frac{1}{2}\left(\frac{G_sJ_s}{dD}+\frac{G_rJ_r}{\ell D}\right)-\frac{1}{2}\left(\nu_y\,\frac{E_sI_s}{dD}+\nu_x\,\frac{E_rI_r}{\ell D}\right)\right]$$

$$+\bar{C}\left\{2\nu_y\left(1+\frac{\nu_x}{2}+\frac{\nu_y}{2}\right)\left[\frac{\bar{S}}{[1+(1-\nu^2)\,\bar{S}]}\left(\frac{t}{\bar{t}_x}\right)^3\left(\frac{\bar{z}_s}{R}\right)\right]\right.$$

$$+2\nu_x\left(1+\frac{\nu_x}{2}+\frac{\nu_y}{2}\right)\left[\frac{\bar{R}}{[1+(1-\nu^2)\,\bar{R}]}\left(\frac{t}{\bar{t}_x}\right)^3\left(\frac{\bar{z}_r}{R}\right)\right]$$

$$\left.-2\left(1+\frac{\nu_x}{2}+\frac{\nu_y}{2}\right)\left[\frac{(1-\nu^2)\,\bar{R}\,\bar{S}(t/\bar{t}_x)^3}{2+2(1+\nu)(\bar{R}+\bar{S})+2\bar{R}\,\bar{S}(1-\nu^2)(1+\nu)}\left(\frac{\bar{z}_r}{R}+\frac{\bar{z}_s}{R}\right)\right]\right\} \qquad (37)$$

Again, it should be noted that in the actual computations of maximum strength, all Poisson ratios are taken equal to $\frac{1}{2}$.

The parameters K and N appear in the Ramberg-Osgood[38] representations of the uniaxial stress-strain curve for aircraft metals; namely,

$$\epsilon = \left(\frac{\sigma}{E}\right) + K\left(\frac{\sigma}{E}\right)^N \qquad (38)$$

As shown in References 10 and 11, the uniaxial stress-strain curve enters the maximum strength analysis through the relacionship

$$\epsilon_{eff} = \left(\frac{\sigma_{eff}}{E}\right) + K\left(\frac{\sigma_{eff}}{E}\right)^{N} \tag{39}$$

The displacement distributions assumed for the imperfect, uniformly shortened shell are

$$u = -ex \tag{40}$$

$$v = 0 \tag{41}$$

$$w_0 = \bar{t}_x \left(\xi_{11_0} \cos\frac{\pi x}{\lambda_x} \cos\frac{\pi y}{\lambda_y} + \xi_{20_0} \cos\frac{2\pi x}{\lambda_x}\right) \tag{42}$$

$$w = \bar{t}_x \left(\xi_{00} + \xi_{11} \cos\frac{\pi x}{\lambda_x} \cos\frac{\pi y}{\lambda_y} + \xi_{20} \cos\frac{2\pi x}{\lambda_x} + \xi_{02} \cos\frac{2\pi y}{\lambda_y}\right) \tag{43}$$

where e, ξ_{11_0}, ξ_{20_0}, λ_x, and λ_y are prescribed, and $\xi_{20_0} = (\xi_{11_0}/4)$ for the calculations.

With no arbitrary parameters appearing in the middle-surface displacements u and v, middle-surface equilibrium is automatically satisfied by the following set of middle-surface stresses:

$$\begin{aligned}\left(\frac{\sigma'_x}{E}\right) = {} & A_{11} \cos\frac{\pi x}{\lambda_x} \cos\frac{\pi y}{\lambda_y} + A_{22} \cos\frac{2\pi x}{\lambda_x} \cos\frac{2\pi y}{\lambda_y} \\ & + 9A_{13} \cos\frac{\pi x}{\lambda_x} \cos\frac{3\pi y}{\lambda_y} + A_{31} \cos\frac{3\pi x}{\lambda_x} \cos\frac{\pi y}{\lambda_y} \\ & + A_{02} \cos\frac{2\pi y}{\lambda_y} - \frac{\sigma}{E}\end{aligned} \tag{44}$$

and

$$\left(\frac{\sigma'_y}{E}\right) = \left(\frac{\lambda_y}{\lambda_x}\right)^2 \left[A_{11} \cos\frac{\pi x}{\lambda_x} \cos\frac{\pi y}{\lambda_y} + A_{22} \cos\frac{2\pi x}{\lambda_x} \cos\frac{2\pi y}{\lambda_y} + A_{13} \cos\frac{\pi x}{\lambda_x} \cos\frac{3\pi y}{\lambda_y} + 9A_{31} \cos\frac{3\pi x}{\lambda_x} \cos\frac{\pi y}{\lambda_y} + A_{20} \cos\frac{2\pi x}{\lambda_x} \right] \tag{45}$$

$$\left(\frac{\tau'_{xy}}{E}\right) = \left(\frac{\lambda_y}{\lambda_x}\right) \left[A_{11} \sin\frac{\pi x}{\lambda_x} \sin\frac{\pi y}{\lambda_y} + A_{22} \sin\frac{2\pi x}{\lambda_x} \sin\frac{2\pi y}{\lambda_y} + 3A_{13} \sin\frac{\pi x}{\lambda_x} \sin\frac{3\pi y}{\lambda_y} + 3A_{31} \sin\frac{3\pi x}{\lambda_x} \sin\frac{\pi y}{\lambda_y} \right] \tag{46}$$

The bending stresses are taken in the form of the curvatures as

$$\left(\frac{\sigma''_x}{E}\right) = a_{11} \cos\frac{\pi x}{\lambda_x} \cos\frac{\pi y}{\lambda_y} + a_{20} \cos\frac{2\pi x}{\lambda_x} + a_{02} \cos\frac{2\pi y}{\lambda_y} \tag{47}$$

$$\left(\frac{\sigma''_y}{E}\right) = \left(\frac{\lambda_y}{\lambda_x}\right)^2 \left[b_{11} \cos\frac{\pi x}{\lambda_x} \cos\frac{\pi y}{\lambda_y} + b_{20} \cos\frac{2\pi x}{\lambda_x} + b_{02} \cos\frac{2\pi y}{\lambda_y} \right] \tag{48}$$

$$\left(\frac{\tau''_{xy}}{E}\right) = \left(\frac{\lambda_y}{\lambda_x}\right) \left[c_{11} \sin\frac{\pi x}{\lambda_x} \sin\frac{\pi y}{\lambda_y} \right] \tag{49}$$

The modified Reissner functional has now been cast in terms of 17 free parameters; ξ_{00} is obtainable from enforcement of the periodicity condition on the v displacement. The vanishing of the first variation of the Reissner functional leads to 17 equations in the 17

unknowns. For a given material (K,N), geometry $(R/\bar{t}_x)$, and prescribed values of e, ξ_{11_0}, $\mu = \lambda_x/\lambda_y$, and $\eta = n^2\bar{t}_x/R$, a load-shortening relationship in the form $\sigma R/E\bar{t}_x$ versus $eR/\bar{t}_x$ can be obtained; the load-shortening curve possesses a distinct maximum except for cylinders in which the maximum amplitudes of the initial imperfection pattern are unreasonably large. For the linear elastic case, the system can be reduced to four equations in the four unknowns ξ_{11}, ξ_{20}, ξ_{02} and (σ/E).

APPENDIX II

STRESS-STRAIN CURVE NONLINEARITY: A POSSIBLE CAUSE OF SCATTER IN TEST RESULTS FOR BUCKLING OF CYLINDERS IN COMPRESSION

The large amount of scatter that exists in plots of experimental buckling stress coefficient $\sigma R/Et$ versus radius-to-thickness ratio R/t is illustrated in Figure 3. The scatter band shown encompasses the extensive data accumulated in References 25 and 46. The lower bound to the data of Reference 25 is given by the empirical relation developed by Weingarten *et al.* in Reference 25; namely,

$$C = \frac{\sigma R}{Et} = 0.606 - 0.546 \left\{ 1 - \exp \left[- \frac{1}{16} \sqrt{\frac{R}{t}} \right] \right\} \qquad (50)$$

where the first term on the right-hand side represents the classical buckling stress coefficient $\left[1/\sqrt{3(1-\nu^2)} \right]$ for Poisson's ratio $\nu = 0.30$.

A modified relation is suggested for present purposes as

$$C = \frac{\sigma R}{Et} = 0.606 - 0.546 \left\{ 1 - \exp \left[- \frac{10^{-5}}{3} \left(\frac{R}{t} \right) \frac{1}{\epsilon_{pl}} \right] \right\} \qquad (51)$$

Equation (51) corresponds closely to the scatter band of Figure 3 at the limits $\epsilon_{pl} = 0.001$ and $\epsilon_{pl} = 0.007$. Aircraft structural metals in general possess proportional limit strains in the range $0.001 < \epsilon_{pl} < 0.007$. Equation (51) can be recast to include the parameters used by Donnell[13] in 1934 in the form

$$C = \frac{\sigma R}{Et} = 0.606 - 0.546 \left\{ 1 - \exp \left[- \frac{10^{-5}}{3} \left(\frac{R}{t} \right) \left(\frac{E}{\sigma_y} \right) \left(\frac{\sigma_y}{\sigma_{pl}} \right) \right] \right\} \qquad (52)$$

For reference, Donnell's design equation taken from Reference 13 is

$$\frac{\sigma R}{Et} = \frac{\left[0.6 - 10^{-7}\,(R/t)^2\right]}{\left[1 + 0.004\,(E/\sigma_y)\right]} \tag{53}$$

It can be observed that Equation (52) includes one more parameter, σ_y/σ_{pl}, than does Equation (53). When the ratio σ_y/σ_{pl} approaches unity, only the parameters perceived by Donnell appear. For σ_y/σ_{pl} approaching unity, however, the equations cannot be compared in general, since they plot with opposite curvatures. Normally, for aircraft materials, the ratio σ_y/σ_{pl} is about 4/3 or greater.

For several values of ϵ_{pl}, Equation (51) is plotted in Figure 3. It can be seen that the scatter band is traversed at any R/t ratio as a function of material nonlinearity. If it is assumed that Donnell's brass cylinders possessed an ϵ_{pl} of 0.0015 (it is known that the yield stress was only about 27 ksi) contrasted with $\epsilon_{pl} \simeq 0.003$ for the Dural cylinders, then the spread between the two curves correlates very well with the actual average behavior of the 21 brass and 45 Dural test cylinders for the range $300 < R/t < 1500$ (see Reference 13).

The strong influence of material nonlinearity indicated by the developments in this appendix cannot be overlooked in attempts to explain the large scatter present in test data for axial compression buckling of thin shells. The scatter heretofore has been attributed principally to initial imperfections through theoretical analyses involving linear material behavior. It appears, however, that the question has not been answered as to just how much influence on scatter may result from material nonlinearity. After all, as Donnell suggested almost 40 years ago, the buckling (or failing) stress of an imperfect thin cylinder in compression should be a function of the yield stress. The contention herein, as well as in the forerunning studies by Mayers and Wesenberg,[10,11] is that buckling (or failure) of an imperfect compressed cylinder is a function of material nonlinearity at stresses

well below the yield stress, especially in the range of "effectively thick" cylinders typical of closely stiffened and sandwich construction.